Damped oscillations of two interacting coronal loops

I. Arregui[1], J. Terradas[1,2], R. Oliver[1] and J. L. Ballester[1]

[1]Departament de Física, Universitat de les Illes Balears, E-07122 Palma de Mallorca, Spain
email: [inigo.arregui, jaume.terradas, ramon.oliver, dfsjlb0]@uib.es

[2]Centrum voor Plasma Astrofysica, K.U. Leuven, Celestijnenlaan 200B, B-3001 Heverlee, Belgium

Abstract. We present results on the oscillatory properties (periods, damping rates, and spatial distribution of perturbations) for resonantly damped oscillations in a system of two inhomogeneous coronal slabs and compare them to the properties found in single slab loop models. A system of two identical coronal loops is modelled, in Cartesian geometry, as being composed by two density enhancements. The linear magnetohydrodynamic (MHD) wave equations for oblique propagation of waves are solved and the damping due to resonant absorption is computed. Due to the interaction between the loops, the normal modes of oscillation present in a single slab split into symmetric and antisymmetric oscillations when a system of two identical slabs is considered. The frequencies of these solutions may differ from the single slab results when the distance between the loops is of the order of a few slab widths. Oblique propagation of waves weakens this interaction, since solutions become more confined to the edges of the slabs. The damping is strong for surface-like oscillations, while sausage body-like solutions are unaffected.

Keywords. MHD, Sun: corona, Sun: magnetic fields, waves

1. Introduction

In the last years, particular attention has been devoted to the phenomenon of transversal coronal loop oscillations, first observed by instruments on-board TRACE spacecraft (Aschwanden et al. 1999; Nakariakov et al. 1999; Aschwanden et al. 2002; Schrijver et al. 2002). The characteristic periods are of the order of minutes and oscillations are quickly damped in a few periods. They have been interpreted by Nakariakov et al. (1999) as the fundamental fast MHD kink mode of a flux tube. The identification of observed oscillations with theoretical MHD wave solutions is the key for coronal seismology, first suggested by Uchida (1970); Roberts et al. (1984) and recently applied by Nakariakov & Ofman (2001); Goossens et al. (2002); Andries et al. (2005); Verwichte et al. (2006); Arregui et al. (2007a), for example. As for the nature of the damping mechanism(s) there is little consensus yet and several mechanisms are currently under study. Resonant conversion of wave energy (Hollweg & Yang 1988; Ruderman & Roberts 2002; Goossens et al. 2002, 2006) is a viable mechanism and is the one considered here.

Observations very often show the excitation and damping of motions in groups of coronal loops rather than in single, isolated structures (see for example Verwichte et al. 2004). However, most of the theoretical models are based on single loop models. For this reason, it is important to fully understand the theoretical properties of MHD waves in multiple-loop structures, to see under which conditions these differences in the oscillatory properties are important and, if important, to make reliable predictions and determinations of unknown physical parameters in the corona.
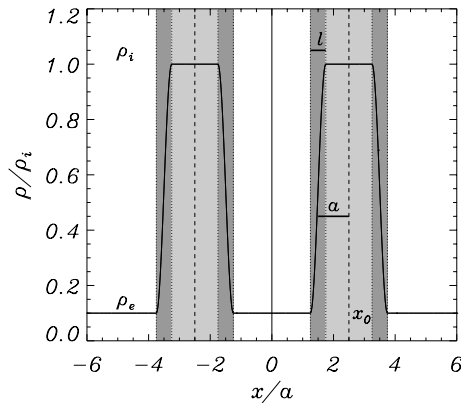
Figure 1. Schematic representation of the two density enhancements (light-shaded regions) of half-width a, centred at $\pm x_0$ representing a system of two coronal slabs in the direction transverse to the equilibrium magnetic field. These enhancements with internal density ρ_i connect to the external medium, with density ρ_e, by transitional non-uniform layers (shaded regions) of thickness l.

In this paper, we present the oscillatory properties of fast MHD waves in a system of two Cartesian slabs when both oblique propagation of perturbations and transversal inhomogeneity of the medium are included.

2. Equilibrium Model, Linear MHD Waves, and Numerical Method

We consider a system of two identical coronal loops as a one-dimensional model in Cartesian geometry. The magnetic field is straight and pointing in the z-direction, $\mathbf{B} = B\,\mathbf{e_z}$. For applications to the solar corona, it is a good approximation to consider that the magnetic pressure dominates over the gas pressure. This classic zero plasma-β limit implies that the magnetic field is uniform and that the density, $\rho(x)$, or Alfvén speed, $v_A(x)$, profiles can be chosen arbitrarily. The system is then modelled by defining a particular equilibrium density profile in the x-direction (see Figure 1), with two density enhancements of half-width a located at $\pm x_0$. The density in each of the slabs is uniform, ρ_i, and connected to the uniform coronal environment, with density ρ_e, by transitional non-uniform layers of thickness l.

The linear resistive MHD equations, with constant magnetic diffusivity, η, are considered. A spatial and temporal dependence of the form $\exp^{i(\omega t - k_y y - k_z z)}$ is assumed for all perturbed quantities, with $\omega = \omega_R + i\omega_I$ the complex frequency and k_y and k_z the perpendicular and parallel wavenumbers. The photospheric line-tying effect is then included by selecting the appropriate parallel wavenumber. This leads to a set of ordinary differential equations for the two components of the velocity perturbation, v_x and v_y, and the three components of the perturbed magnetic field, b_x, b_y, and b_z. As the plasma-$\beta=0$, the slow mode is absent and $v_z = 0$. Numerical approximations to the solutions are obtained using PDE2D (Sewell 2005), a general-purpose partial differential equation solver. As for the boundary conditions, we impose the vanishing of the perturbed velocity far away from the two-slab system, hence $\mathbf{v} \to 0$ as $x \to \pm\infty$.
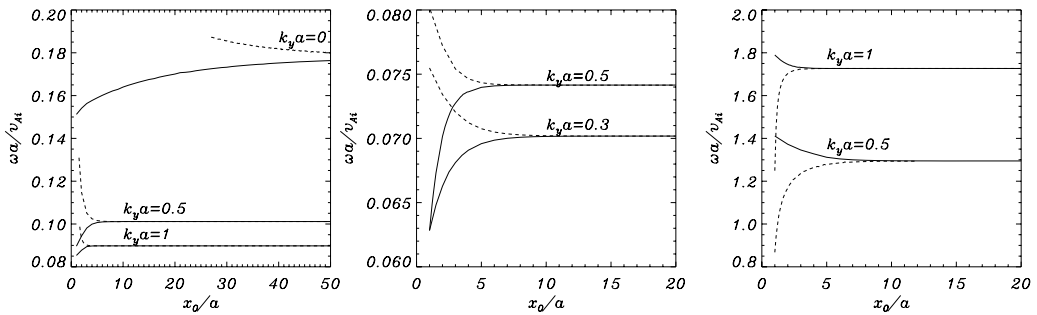
Figure 2. Frequency as a function of the position of the slabs centres for different values of the perpendicular wavenumber for the kink solutions (*left*), the sausage surface solutions (*middle*), and the sausage body solutions (*right*).

3. Analysis and Results

When $k_y = 0$ and $l = 0$, Luna et al. (2006) find that the kink transversal oscillation of a single slab splits into symmetric and antisymmetric solutions with respect to $x = 0$. In the limit of no separation between slabs, the symmetric mode frequency is equal to the kink mode frequency of a single slab with double width. As the distance between the slabs is increased, the interaction weakens and, for large separations, the frequency of the whole system goes to the kink mode frequency of a single slab. When compared to Luna et al. (2006), two new ingredients are included in this paper; the non-uniformity of the equilibrium density and perpendicular propagation of perturbations. These two ingredients produce the resonant damping of fast modes.

When only oblique propagation of waves ($k_y \neq 0$, $l = 0$) is considered solutions can be obtained by solving an analytical dispersion relation. Arregui et al. (2007b) have shown, for a single Cartesian slab, that the fundamental kink mode, which is body for values of k_y below certain value, becomes surface beyond that particular value. There is a sausage surface wave, with its frequency always below the internal cut-off frequency, which only exists when $k_y \neq 0$. The phase speed of these two solutions goes asymptotically to the kink speed for quasi-perpendicular propagation ($k_y \gg k_z$). The sausage body solution, which is leaky in the long wave limit ($k_z a \ll 1$), becomes trapped when a non-zero k_y is included. This solution is always above the internal cut-off frequency and, hence, keeps its body character in the limit of quasi-perpendicular propagation. When a second density enhancement is included, the solutions described by Arregui et al. (2007b) split into symmetric and antisymmetric solutions with respect to $x = 0$, giving six solutions. Consider fixed values for the density contrast of the two-slab system, $\rho_i/\rho_e = 10$, and for the longitudinal wavenumber, $k_z a = \pi/50$. In Figure 2 we can clearly see that for the kink symmetric and antisymmetric solutions, the range of distances for which the interaction is strong and the deviation from the kink mode frequency of a single slab significant, is large in the absence of perpendicular propagation ($k_y = 0$). When perpendicular propagation is included the single slab kink mode frequency is approached for much smaller distances between slabs. Only for distances of the order of a few times a the symmetric and antisymmetric solutions have frequencies that differ significantly from the kink frequency of a single slab. As for the sausage surface and sausage body, symmetric and antisymmetric solutions, a similar result is obtained regarding the splitting of the single slab solutions and the deviation from the single slab frequencies as a function of the slab separation and perpendicular wavenumber. For the kink solutions, and considering for example $x_0 = 2a$, the frequency of the symmetric mode is 15% smaller than the kink
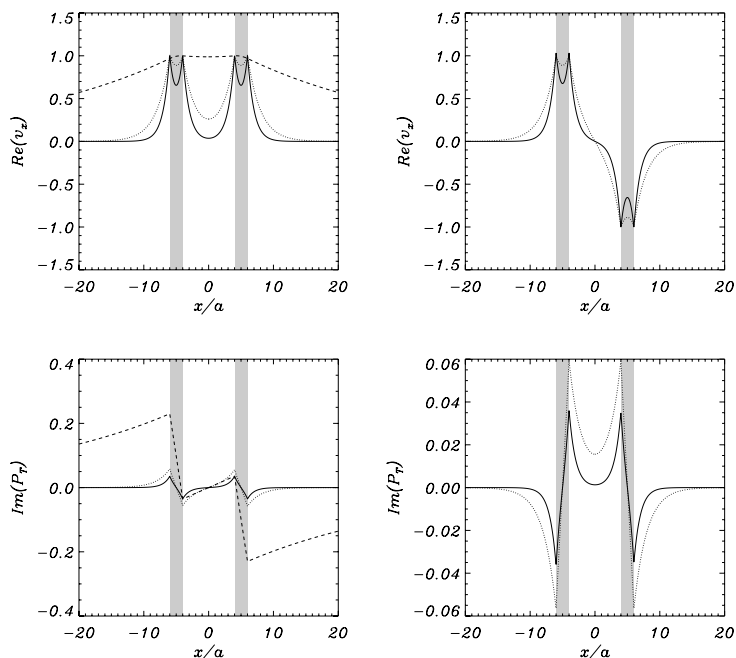
Figure 3. Real part of the transversal velocity component, v_x, and imaginary part of the perturbed total pressure, P_T, for the fundamental symmetric (*left*) and antisymmetric (*right*) kink solutions, for several values of the perpendicular wave number: $k_y a = 0$ (dashed lines), $k_y a = 0.5$ (dotted lines), and $k_y a = 1$ (solid lines). Note that the character of the eigenfunctions for the symmetric mode changes from body-like to surface-like solution as k_y is increased. In all figures the light-shaded regions represent the density enhancements. These solutions have been obtained with a uniform computational grid with $N_x = 10\,000$ points in the range $-80 \leqslant x/a \leqslant 80$ (except for the kink solutions with $k_y = 0$ for which a range $-200 \leqslant x/a \leqslant 200$ has been used).

mode frequency of a single slab, when $k_y = 0$. This difference decreases to 3% for $k_y a = 1$. When the two-slab system is oscillating in the antisymmetric mode, its frequency is 13% larger that the kink mode frequency for $k_y a = 0.5$, while it is only 4% for $k_y a = 1$. As for the sausage surface solutions of the two-slab system, a deviation from the sausage surface frequency of a single slab around 5% is found, in the case of the symmetric solution with $k_y a = 0.3$ and $x_0 = 2a$. Finally, for the sausage body solutions of the two-slab system with $x_0 = 2a$, the maximum difference occurs for the antisymmetric solution with $k_y a = 0.5$ and is around 10%.

Figures 3, 4, and 5 show the transversal component of the perturbed velocity and the total pressure perturbation for the kink, sausage surface, and sausage body, symmetric and antisymmetric solutions, for different values of the perpendicular wavenumber. When oblique propagation is included, there is an improved confinement of the eigenfunctions with a sharper drop-off rate in the external medium, a behaviour first found by Díaz et al. (2003), in the context of prominence fibril oscillations. The character of the solutions inside the slabs change, becoming surface-like solutions, with a decreasing amplitude of v_x inside the slabs as k_y is increased. This improved confinement of the solutions weakens the interaction between the slabs. In Figures 4 and 5, we can appreciate that sausage surface and body solutions have a similar spatial distribution of eigenfunctions. The main difference is in the total pressure perturbation profiles. An increase in the perpendicular wavenumber also produces an improved confinement, in the external regions, for these
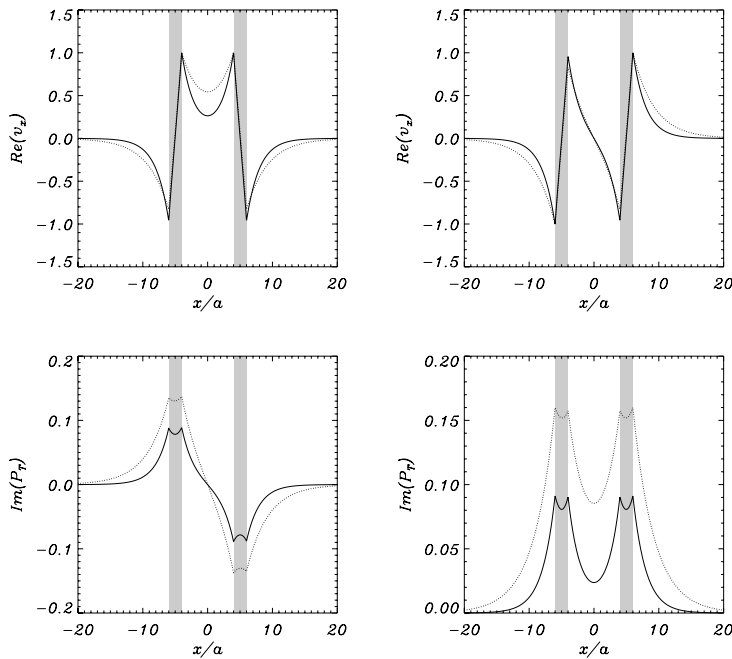
Figure 4. Same as Figure 3 for the sausage surface, symmetric (*left*) and antisymmetric (*right*) solutions and two values of the perpendicular wavenumber: $k_y a = 0.3$ (dotted lines) and $k_y a = 0.5$ (solid lines). These solutions are surface-like for all values of the perpendicular wavenumber.

four types of modes, but in contrast to the kink solutions, now the transversal velocity component inside the slabs is not affected by the increase in k_y and the solutions keep their surface or body character.

To study the damping of the normal modes described previously, we now include non-uniform transitional layers at the edges of each slab ($l \neq 0$). For the normal mode analysis a small but finite value of the resistivity has to be provided when computing the damping of oscillations. Figure 6 displays the damping per period of the six solutions as a function of the perpendicular wavenumber, for a fixed value of the distance between the slabs. For increasing k_y, the damping for both symmetric and antisymmetric solutions approaches the damping of the kink, sausage surface, and sausage body solutions of a single slab, in the limit of quasi-perpendicular propagation. Surface-like solutions, kink and sausage alike are strongly damped, within a few periods, for large values of k_y, while sausage body solutions are unaffected by resonant couplings (see Figure 6, bottom row). The reason is that the frequencies of sausage body modes lie outside the corresponding Alfvén continua. The difference in damping for the symmetric mode with respect to the kink mode damping of a single slab is below 10%. The kink antisymmetric solution damping is more than double that of the kink mode of a single slab. Also significant are the differences between the sausage surface symmetric and antisymmetric damping and the corresponding sausage surface mode damping of a single slab. The imaginary parts for these two modes are 70% smaller and larger, respectively, than the value for the single slab mode.
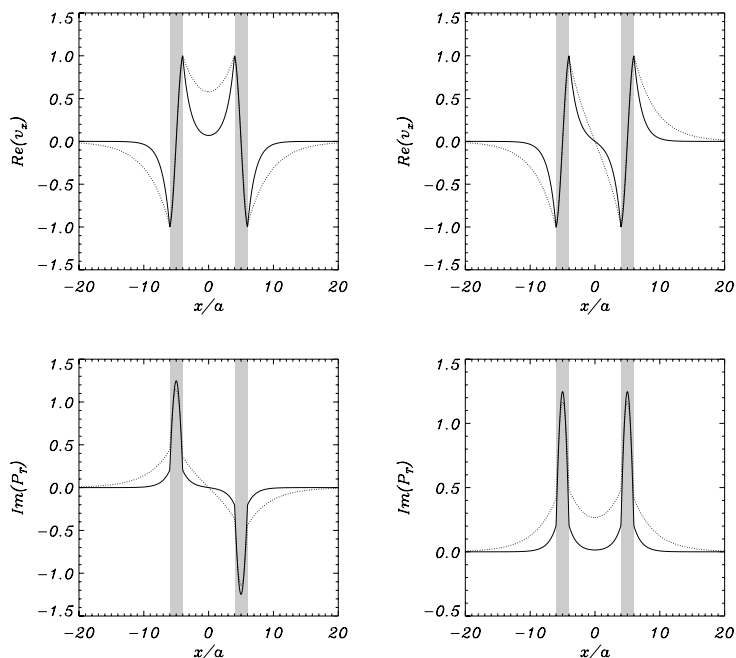
Figure 5. Same as Figures 3 and 4 for the sausage body, symmetric (*left*) and antisymmetric (*right*) solutions and two values of the perpendicular wavenumber: $k_y a = 0.5$ (dotted lines) and $k_y a = 1$ (solid lines). Note that for these solutions v_x is very similar to the ones depicted in Figure 4, while the pressure perturbation in and around the slabs differ substantially. These solutions are body-like for all values of the perpendicular wavenumber.

4. Summary and Conclusions

The normal modes of oscillation in a two-slab system are, in general, different to those of a single and isolated slab, due to the interaction between the slabs. The single slab fast kink and sausage normal modes split into symmetric and antisymmetric solutions. The frequencies of these solutions are in general different from the single slab solutions. They depend upon the distance between the slabs, but also on the magnitude of the perpendicular wavenumber. The inclusion of oblique propagation of perturbations introduces two new surface-like solutions, with sausage parity. It also decreases the effect of the interaction between the slabs, since solutions are more confined to the neighbourhood of the density enhancements. Both the distance between slabs and perpendicular propagation determine the difference in frequency between the single slab model solutions and the modes described in this paper. These differences are of the order of 15% at most and should, therefore, be taken into account in the modelling of these events. They are, however, well below the observational uncertainties, which are of the order of 40% (Aschwanden et al. 2002). Surface-like solutions, both kink and sausage, are strongly damped. On the other hand, the two sausage body solutions are unaffected by resonant absorption. A comparison with the single slab model results reveals that differences in damping are important for small values of the distance between the slabs. The most significant differences arise for the kink antisymmetric solution and the two sausage surface solutions, with differences in the imaginary part of the frequency of the order of 125% and 70% with respect to the damping of the corresponding single slab modes. These
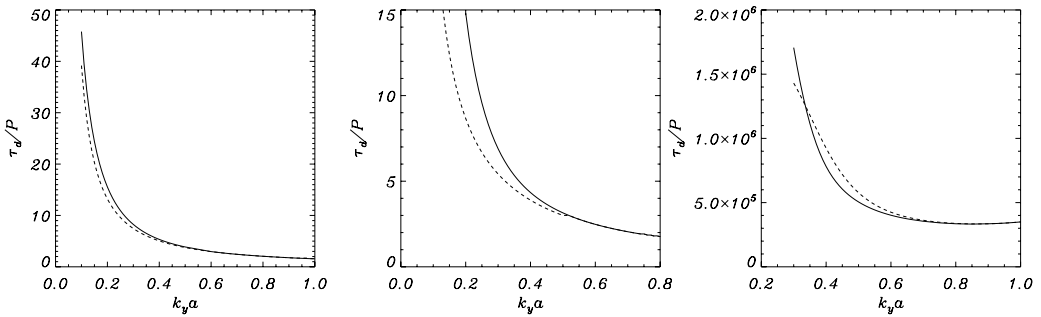
Figure 6. Damping time over period as a function of the perpendicular wavenumber for the same six types of solution, for the same parameter values and a fixed distance between the slabs, $x_0 = 5a$. In all the figures the solid lines correspond to the symmetric solution and the dashed lines to the antisymmetric solution. A value for the magnetic Reynolds number $R_m = v_{Ai}a/\eta = 10^7$ has been used in a non-uniform grid with $N_x = 14\,000$ points (2 000 in each of the four non-uniform transitional layers) in the range $-80 \leqslant x/a \leqslant 80$.

differences are of the order or larger than the observational uncertainties for the measured damping times in, which are around 60% (Aschwanden et al. 2002).

Acknowledgements

References

Andries, J., Arregui, I., & Goossens, M. 2005, ApJ, 624, L57
Arregui, I., Andries, J., Van Doorsselaere, T., Goossens, M., & Poedts, S. 2007a, A&A, 463, 333
Arregui, I., Terradas, J., Oliver, R., & Ballester, J. L. 2007b, Solar Phys., in press, DOI 10.1007/s11207-007-9041-3
Aschwanden, M. J., De Pontieu, B., Schrijver, C. J., & Title, A. M. 2002, Solar Phys., 206, 99
Aschwanden, M. J., Fletcher, L., Schrijver, C. J., & Alexander, D. 1999, ApJ, 520, 880
Díaz, A. J., Oliver, R., & Ballester, J. L. 2003, A&A, 402, 781
Goossens, M., Andries, J., & Arregui, I. 2006, Phil. Trans. Series A, 364, 433
Goossens, M., Andries, J., & Aschwanden, M. J. 2002, A&A, 394, L39
Hollweg, J. V. & Yang, G. 1988, J. Geophys. Res., 93, 5423
Luna, M., Terradas, J., Oliver, R., & Ballester, J. L. 2006, A&A, 457, 1071
Nakariakov, V. M. & Ofman, L. 2001, A&A, 372, L53
Nakariakov, V. M., Ofman, L., DeLuca, E. E., Roberts, B., & Davila, J. M. 1999, Science, 285, 862
Roberts, B., Edwin, P. M., & Benz, A. O. 1984, ApJ, 279, 857
Ruderman, M. S. & Roberts, B. 2002, ApJ, 577, 475
Schrijver, C. J., Aschwanden, M. J., & Title, A. M. 2002, Solar Phys., 206, 69
Sewell, G. 2005, The Numerical Solution of Ordinary and Partial Differential Equations (Wiley-Interscience)
Uchida, Y. 1970, Pub. Astron. Soc. Japan, 22, 341
Verwichte, E., Foullon, C., & Nakariakov, V. M. 2006, A&A, 452, 615
Verwichte, E., Nakariakov, V. M., Ofman, L., & Deluca, E. E. 2004, Solar Phys., 223, 77